Prostaphopain B Structure: A Comparison of Proregion-Mediated and Staphostatin-Mediated Protease Inhibition[†,‡]

Renata Filipek,[§,||,⊥] Roman Szczepanowski,[§,||] Artur Sabat,[⊥] Jan Potempa,[⊥,@] and Matthias Bochtler*[,§,||]

International Institute of Molecular and Cell Biology, ul. Trojdena 4, 02-109 Warsaw, Poland, Max-Planck-Institute for Molecular Cell Biology and Genetics, Pfotenhauerstrasse 108, 01309 Dresden, Germany, Faculty of Biotechnology, Jagiellonian University, Gronostajowa 7, 30-387 Kraków, Poland, and Department of Biochemistry and Molecular Biology, University of Georgia, Athens, Georgia 30602

Received June 26, 2004; Revised Manuscript Received August 27, 2004

ABSTRACT: Prostaphopain B is the precursor of staphopain B, a papain-type secreted cysteine protease from the pathogen *Staphylococcus aureus*. Here, we describe the 2.5 Å crystal structure of the proenzyme. Its 21 kDa proregion is organized around a central half-barrel or barrel-sandwich hybrid and occludes primed, but not nonprimed, sites in the active site cleft of the protease. The structure of the mature part of the protease is similar to previously reported staphopain structures, and no distortion of the catalytic residues is apparent at 2.5 Å resolution. A comparison of prostaphopain B with the staphopain B−staphostatin B complex shows that the proregion and the inhibitor interact with largely nonoverlapping parts of the protease surface. In a modeled complex of prostaphopain B with staphostatin B, clashes occur both inside and outside the active site cleft, but involve mostly poorly ordered regions of the protein that may be mobile.

Many papain-type (Clan CA) cysteine peptidases are produced as inactive proenzymes that require cleavage of their N-terminal inhibitory proregions for activation. The proregions of papain-type cysteine peptidases are poorly conserved and often structurally unrelated (*1*). Although all proregions quench the proteolytic activity of the mature enzymes, the specific inhibition mechanisms vary. Occlusion of the substrate binding cleft (*2*−*7*), engagement of the active site cysteine in a disulfide bridge (*8*), and displacement of the catalytically essential histidine residue (*9*) have all been described for proforms of papain-type enzymes.

Staphopains A and B (also known as ScpA and SspB, respectively), the major secreted staphylococcal cysteine peptidases, are papain-type enzymes. Their genes encode preproenzymes that consist of a leader peptide, a 21 kDa proregion, and the 20 kDa mature enzyme. The similarity between mature staphopain B and other papain-type peptidases is readily apparent from multiple-sequence alignments (data not shown). In contrast, we could not detect significant homologues of the proregions of prostaphopains A and B among the proregions of other papain-type cysteine peptidases. The 20.8 kDa molecular mass of the prostaphopain B proregion is remarkable. It is significantly greater than the molecular mass of the proregions of all structurally characterized papain-type enzymes and slightly greater than the molecular mass of mature staphopain B.

Maturation of both staphopains A and B involves several steps. Intracellularly, both are expected to be present as preproenzymes. Cleavage of the leader peptide should occur concomitantly with secretion. Maturation is thought to occur extracellularly and, in case of staphopain B, depends on the presence of V8 protease in the supernatant (*10*, *11*).

Staphopain B is the target for staphostatin B, the product of the *sspC* gene. Although there is consensus in the literature that staphostatin B inhibits staphopain B, the detailed properties of staphostatin B are controversial (*10*, *11*). Massimi and colleagues reported the detection of a complex between staphostatin B and prostaphopain B (*10*). They proposed that staphostatin B serves to maintain prostaphopain B latency. According to their model, activation of prostaphopain B requires V8 protease to cleave off the proregion and to inactivate staphostatin B (*10*). As V8 protease is located in the extracellular space, this model requires that staphostatin B be coexported with prostaphopain B.

In contrast to Massimi *et al*., Rzychon *et al*. could not detect a complex between prostaphopain B and staphostatin B, although they obtained a very tight, stoichiometric complex between staphostatin B and mature staphopain B (*11*). Moreover, these authors were able to demonstrate the presence of the inhibitor in *Staphylococcus aureus* lysates, but not in extracellular fractions of *S. aureus* cultures. In line with these findings, Rzychon *et al*. suggested that staphostatin B remains intracellular and serves as a "second backup" against premature staphopain activation (*11*).

[†] This work was done with financial support from KBN, The State Committee for Scientific Research (1789/E-529/SPB/5.PR UE/DZ 600/2002−2005, 158/E-338/SPB/5.PR UE/DZ 19/2003, and KO89/PO4/2004), and from the Commission of the European Communities, specific RTD programs "Quality of Life and Management of Living Resources" (QLRT-2001-01250) and "Novel non-antibiotic treatment of staphylococcal diseases".

[‡] Coordinates and structure factors have been submitted to the Protein Data Bank as entry 1X9Y.

* To whom correspondence should be addressed. E-mail: MBochtler@iimcb.gov.pl. Telephone: 0048 22 6685193. Fax: 0048 22 6685288.

[§] International Institute of Molecular and Cell Biology.

[||] Max-Planck-Institute for Molecular Cell Biology and Genetics.

[⊥] Jagiellonian University.

[@] University of Georgia.

10.1021/bi048661m CCC: $27.50
Published on Web 10/16/2004

We have previously determined the crystal structures of free staphostatin B (*12*) and of staphostatin B in complex with mature staphopain B (*13*). These studies have confirmed the expected structural similarity between mature staphopain B and other papain-type cysteine peptidases, especially staphopain A. Moreover, we have shown that staphostatins represent a novel class of cysteine peptidase inhibitors that insert their binding loops in substrate-like direction into the active site clefts of their target proteases. Here, we extend our previous studies and report the crystal structure of prostaphopain B. The crystal structure shows that the mechanism that maintains prostaphopain B latency differs from previously described mechanisms that ensure proenzyme latency in other papain-type cysteine peptidases. Moreover, the crystal structure suggests a possible explanation for discrepancies in the literature about the prostaphopain B−staphostatin B interaction.

EXPERIMENTAL PROCEDURES

Prostaphopain B Cloning, Expression, Purification. Prostaphopain B from *S. aureus* strain V8 was cloned into vector pGEX-5T as a glutathione *S*-transferase (GST) fusion protein via *Bam*HI and *Xho*I. Two constructs were prepared, one with the stop codon immediately after the last residue of the open reading frame (named pSsspB-pGEX-5T) and a second one with the stop codon taken from the vector, resulting in the addition of the LEVPIHRD peptide at the C-terminus. *Escherichia coli* BL21(DE3) cells were transformed with the expression construct, grown at 37 °C to an A_{600} of 0.7, induced with 1 mM IPTG,[1] and cooled to 30 °C. Four hours after induction, cells were harvested, resuspended in buffer A [20 mM Tris (pH 7.5) and 50 mM NaCl], and frozen. After thawing, cells were treated with lysozyme and DNase I and opened by sonication. After centrifugation (40 000 rpm for 40 min), the supernatant was applied to glutathione−Sepharose 4B (Amersham Biosciences) at 4 °C. The resin was washed with buffer B [20 mM Tris (pH 7.5) and 200 mM NaCl], and the fusion protein was eluted form the resin with buffer C [10 mM glutathione, 10 mM Tris (pH 8.0), and 50 mM NaCl]. The prostaphopain B−GST fusion was cleaved with thrombin (Sigma, 28 units of thrombin/10 mg of fusion protein) in buffer C with 5 mM $CaCl_2$ for 5−7 days at 4 °C. Because of the specificity of thrombin, the proenzyme bears the Gly-Ser N-terminal extension. After gel filtration on Sephacryl S-300 column (Amersham Biosciences) in 5 mM Tris (pH 7.5) to remove glutathione, GST and remaining noncleaved material were scavenged with glutathione−Sepharose 4B resin, and the enzyme was concentrated to 15−20 mg/mL by ultrafiltration (VivaSpin, VivaScience, 10 kDa cutoff).

Prostaphopain B Proregion Cloning, Expression, and Purification. Fragments encoding the proregion were amplified by standard PCR from the proSspB expression construct (pSsspB-pGEX-5T) and from genomic DNA of *S. aureus* NCTC 8325-4 with primers 5′-GGAATTCCATATGAAACAGCTAGAAATTAATG-3′ and 5′-AAGGATCCTCGAGTCAAACTTTTGTAGGTGTTAC-3′. The 530 bp amplicons were cloned via *Eco*RI and *Xho*I into a derivative of pET15b (Novagen), named pET15bmod, which lacks the original *Eco*RI site and contains a newly introduced *Eco*RI site in place of the original thrombin cleavage site. Thus, the N-terminal sequence of our construct was MGHHHHHHEFHMKQLE..., where the KQLE segment constitutes the first residues of the native proregion of the prostaphopain B sequence and the PTKV segment the last ones. The D98H mutation was introduced into the expression construct for the proregion of prostaphopain B from strain V8 by site-directed mutagenesis according to the QuickChange protocol with *PfuTurbo* DNA polymerase (Stratagene).

For the expression of both wild-type and mutant proregions in *E. coli*, BL21(DE3) cells were transformed with the appropriate expression constructs, grown at 37 °C to an A_{600} of 1.0, induced with 0.5 mM IPTG, and shifted to 28 °C for 4 h. Cells were harvested by centrifugation, resuspended in buffer A, and frozen. After thawing, cells were treated with lysozyme and DNase I at 4 °C and disrupted by sonication. The soluble fraction was separated by ultracentrifugation, and the supernatant was applied to a nickel−NTA agarose (Qiagen) column. The column was washed with 30 mM imidazole in buffer D [20 mM Tris (pH 7.5) and 100 mM NaCl] and eluted with 100 mM imidazole in buffer A. The eluate was concentrated and applied to a Sephacryl S-200 (Pharmacia) gel filtration column in buffer A. The eluate was concentrated on Amicon (Millipore) 10 kDa cutoff regenerated cellulose filters.

Mature Staphopain B Cloning, Expression, and Purification. Staphopain B for biochemical assays was purified from the native source according to the published protocol (*13*). The inactive mutant of staphopain B (C243A) (*13*) was subcloned via *Nde*I and *Xho*I into pET14b (Novagen). For protein expression, BL21(DE3) cells were freshly transformed with the expression construct and grown at 37 °C to an A_{600} of 1.0 and, after induction with 0.5 mM IPTG, were cooled to 28 °C for 5 h. Up to the elution from the nickel−NTA agarose (Qiagen) column, all purification steps were identical to those of the proregion purification. In the staphopain B purification, the eluate was concentrated to 10 mg/mL and the His tag was cleaved with thrombin (Sigma) at 4 °C for 2−4 days. After the cleavage was completed, the protein was applied to a Sephacryl S-200 (Pharmacia) gel filtration column in buffer A. The eluate was concentrated on Amicon (Millipore) 10 kDa cutoff regenerated cellulose filters.

Staphostatin B Expression and Purification. Staphostatin B was recombinantly expressed in *E. coli* and purified as described previously (*11*). For all proteins, the protein concentration was calculated from the absorbance at 280 nm, using amino acid composition-based extinction coefficients. The purity and identity of all proteins were assessed by SDS−PAGE and mass spectrometry.

Size Exclusion Chromatography. Analytical gel filtration runs were performed with a Superdex 75 PC 3.2/30 column (Amersham Biosciences) (see Figure 4A and Figures 6A and 6B) or a Superose 12 HR 10/30 column (Amersham Biosciences) (see Figure 6C) in buffer containing 50 mM Tris (pH 7.5), 150 mM NaCl, 2 mM DTT, and 1 mM EDTA at 4 °C. For complex formation, the proteins were mixed in

[1] Abbreviations: Abz, 2-aminobenzoyl; Bz, benzoyl; Dnp, 2,4-dinitrophenyl; E-64, L-*trans*-epoxysuccinyl-leucylamido(4-guanidino)-butane; EDTA, ethylenediamine-*N*,*N*,*N*′,*N*′-tetraacetic acid; IPTG, isopropyl thio-β-D-galactopyranoside; pNA, *p*-nitroanilide; PEG, polyethylene glycol; SspB, staphylococcal cysteine protease B.

equimolar amounts (8 nmol) in column equilibration buffer and incubated at 4 °C for 20 min. The recombinant inhibitor (staphostatin B), proenzyme (prostaphopain B), and inactive mutant of mature protease (staphopain B C243A), all from strain V8, and proregions from strains V8 and NCTC 8325-4 (identical to the proregion from strain SP6391) were used in this study. The proregions from both strains behave similarly in all gel filtration runs.

Determination of Binding Constants. The proregion of prostaphopain B acts as an inhibitor of the mature protease if supplied in trans. The affinity between the two components was therefore measured according to a procedure previously developed for the staphopain B−staphostatin B interaction with the fluorescence-quenched substrate Abz-Gln-Gly-Ile-Gly-Thr-Ser-Arg-Pro-Lys(Dnp)-Asp-OH in 20 mM Tris (pH 7.5) in the presence of 2 mM cysteine and 5 mM EDTA (*13*). Assays were carried out in a 300 μL reaction volume with either 50 or 100 nM staphopain B and 1 μM substrate, a concentration significantly lower than the K_m. Initial hydrolysis rates were determined as a function of proregion concentration. The assays with Bz-Pro-Phe-Arg-pNA were carried out according to the published protocol (*10*).

Prostaphopain B Crystallization and Data Collection. The prostaphopain B variants with and without the additional residues at the C-terminus from the expression vector were used for extensive crystallization trials, but only the form with extra residues at the C-terminus could be crystallized. Crystals were grown in sitting drops at 21 or 4 °C by equilibrating a 1:1 mixture of the protein [~15 mg/mL in 5 mM Tris (pH 7.5)] and reservoir buffer against reservoir buffer containing 50 mM Bis-Tris (pH 6.5), 20% (w/v) PEG 4K or 100 mM HEPES (pH 7.5), 21% (w/v) PEG 4K, and 10% (v/v) 2-propanol. Thin plates of orthorhombic crystals in space group $P2_12_12_1$ appeared within a few weeks and diffracted to ~2.8 Å in house. Crystals were transferred into a cryoprotecting solution containing a 7:1 mixture of reservoir solution and (2*R*,3*R*)-(−)-2,3-butanediol (Sigma) and then flash-cooled with liquid nitrogen. For most crystals, mosaicity was high and anisotropic, resulting from poor crystal growth in the direction of the long crystallographic axis. Moreover, the length of the long axis varied between 177 and 184 Å at room temperature and between 166 and 180 Å at cryo temperature. Although several data sets were collected at synchrotron beamlines, the best data set to 2.5 Å with good statistics (see Table 1) was obtained from a crystal that was grown at 4 °C, flash-cooled to 100 K in a nitrogen gas stream (Oxford Cryosystem) and annealed once, a procedure that proved to be difficult to repeat, and measured with Cu Kα radiation (Rigaku RU-300 rotating anode generator, MSC) and an image plate detector (MAR345, Mar Research) in house.

Prostaphopain B Structure Determination. The prostaphopain B structure was determined by a combination of molecular replacement and multiple isomorphous replacement. With mature staphopain B (without residues Val329−Leu338) (*13*) as the search model, MOLREP (*14*) yielded a highly tentative molecular replacement solution (*R*-factor = 55%) that could be used to calculate difference Fourier maps for more than 40 heavy atom soaks. On the basis of the difference Fourier maps, two mercury soaks were identified that yielded mercury sites in chemically reasonable environments. After crystals were soaked for 2 days at room temperature with 60 mM potassium thiocyanatomercurate, mercury appeared to bind specifically to a small cavity in the staphopain B structure surrounded by three methionine residues. Crystals that were soaked for 1 day at room temperature with 8 mM sodium ethylmercurithiosalicylate (thiomersal) contained mercury close to the active site cysteines. Probably because of crystal nonisomorphism, both derivatives had useful phasing power only at very low resolution. The resulting maps correlated poorly with the model, but allowed the definition of a solvent mask that was consistent with the molecular boundaries of the four copies of the mature form of the protease and predicted the location of the globular parts of the four copies of the proregion in the asymmetric unit of our crystals. With an averaging mask closely modeled on this experimental observation, 4-fold averaging of a $2F_o - F_c$ map that was calculated with the placed mature forms as input coordinates yielded a map that clearly showed the location of some β-strands and of one long α-helix after skeletonization. In this map, partial models for the four proregions could be built with MAID (*15*), and could be further improved manually by exploiting the 4-fold local symmetry. NCS-phased refinement as implemented in the CCP4i suite (*16*) with this partial model produced a dramatically improved map with clear connectivity even in loops. After another round of MAID to build more secondary structure elements, the sequence could be assigned with confidence and the model completed manually with the modeling program O (*17*). Water picking was done with ARP/WARP (*18*), and final refinement of the structure was carried out with CNS (*19*) applying tight NCS restraints for most of the molecule.

Table 1: Data Collection and Refinement Statistics

Data Collection	
space group	$P2_12_12_1$
a (Å)	84.6
b (Å)	104.9
c (Å)	173.1
no. of independent reflections	53496
resolution (Å)	2.5
completeness (%)	99.1
R_{sym} (%) (last shell)	6.7 (33.9)
I/σ (last shell)	17.0 (3.0)
Refinement	
R-factor (%)	24.4
R_{free} (%)	27.6
rmsd for bond lengths (Å)	0.007
rmsd for bond angles (deg)	1.3
B (isotropic) from Wilson	46.9
Ramachandran core (%)	87.6
Ramachandran additionally allowed regions (%)	12.4
Ramachandran generously allowed regions (%)	0
Ramachandran disallowed regions (%)	0

The final model is consistent with experimentally determined heavy atom positions and packs well in the *a*−*b* plane. The packing in the *c* direction appears to be fragile, and explains the large variation in cell constants between different specimens of this crystal form and the poor crystal growth in this direction. The quality indicators of the data set that was used for final refinement and of the completed model are summarized in Table 1 and appear to be satisfactory. The buried surface area was calculated in CNS with a probe radius of 1.4 Å (*20*).

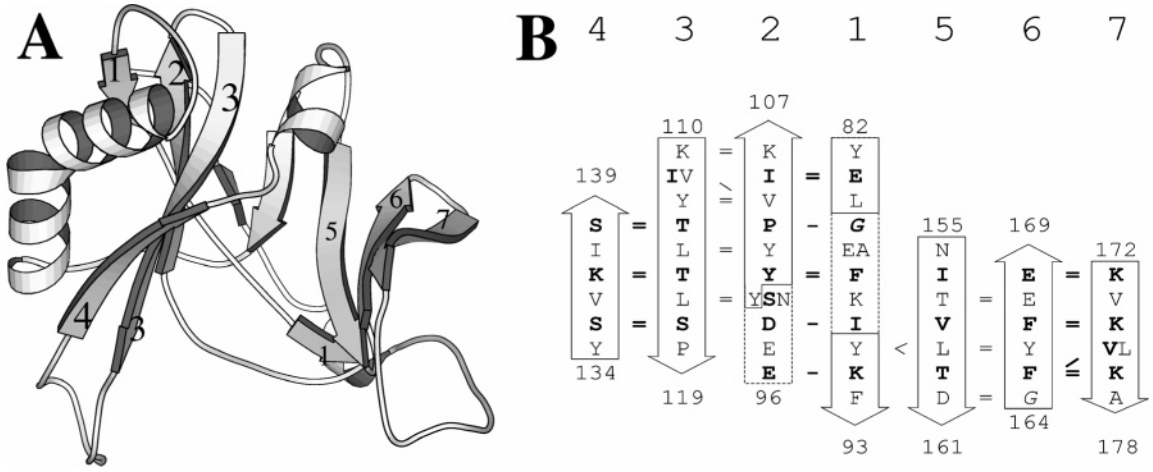

FIGURE 1: Proregion of prostaphopain B. (A) Ribbon representation drawn with MOLSCRIPT, using the DSSP secondary structure assignment without manual corrections. Only strands that are part of the half-barrel or barrel-sandwich hybrid have been numbered. Note that the strong distortion of strand 1 prevents its classification as one continuous strand in DSSP. (B) Schematic representation of the main chain hydrogen bonding arrangement of the half-barrel. Residues that point toward the inside are printed in bold type; residues that point outward are printed in regular type, and glycines and residues that that have the $C^{\alpha}-C^{\beta}$ bond essentially in the plane of the β-sheet are printed in italic type.

RESULTS

Prostaphopain B Expression and Purification. Prostaphopain B from *S. aureus*, strain V8, was recombinantly expressed as a GST fusion protein in *E. coli* and purified by glutathione affinity chromatography and gel filtration. The activity of our preparations was assayed by zymography and, independently, with the chromogenic substrate Bz-Pro-Phe-Arg-pNA (*10*), either with or without prior addition of V8 protease to process the enzyme to its mature form. Without addition of V8 protease, the activity of fresh prostaphopain B preparations was barely detectable. Activity increased upon storage, but in our hands, and in contrast to the results of Massimi *et al*. (*10*), it always remained low by comparison with the activity of the mature protease. Samples that were pretreated with V8 protease migrated faster and showed robust activity in zymography and at least 50-fold higher specific activity than nonpretreated samples in the assay with Bz-Pro-Phe-Arg-pNA (data not shown), strongly suggesting that recombinant prostaphopain B was folded.

Prostaphopain B Crystallization and Structure Determination. Prostaphopain B crystals could be grown in space group $P2_12_12_1$ and diffracted to 2.5 Å resolution. They contained four molecules in the asymmetric unit and were packed very tightly in the $a-b$ plane and very poorly in the c direction. One pair of monomers is displaced from the other pair by one-half of a unit cell along the y axis almost without rotation. The four molecules in the asymmetric unit are highly similar (root-mean-square deviation of 0.03 Å for 300 of the 346 modeled residues in the protein that were subjected to NCS-restrained refinement). Differences are essentially confined to a long loop from residue Asn183 to Leu202 in the proregion and to another loop from Ser328 to Leu338 in the mature form that had to be modeled into poor electron density and appear to adjust to the local crystal environment. Detailed differences are not biologically relevant, but they suggest that these parts of the proenzyme are mobile. This conclusion has important implications for the latency mechanism that will be discussed below.

Proregion Fold. The fold of the prostaphopain B proregion is fairly unusual. A DALI (*21*) quantitative structure comparison of the proregion with all other protein structures currently available from the Protein Data Bank (PDB) failed to detect any known structures with more than marginal similarity (all DALI Z scores < 2.5).[2] In qualitative terms and SCOP (*22*) nomenclature, the prostaphopain B proregion can be approximately described as a "half-barrel" or "barrel-sandwich hybrid", if the two parts of the β-strand that are labeled as "1" in Figure 1A are considered part of one larger continuous strand. The DSSP automatic classification as two strands results from a bifurcation in the structure. As can be seen in Figure 1A, strand "5" accepts and donates hydrogen bonds to the C-terminal part of strand "1" and to a strand that is not part of the half-barrel architecture. This extra strand is part of a three-stranded β-sheet that shields substantial parts of the outer surface of the half-barrel from solvent. The long, kinked helix from residue Gln54 to Gln74 (on the left in Figure 1A) and the linker that covalently connects the proregion to the mature form (only the ordered part is shown in Figure 1A) bury additional surfaces on the outside of the half-barrel. In contrast, the "open" nature of the half-barrel leaves the interior unusually exposed to solvent. With the exception of a prominent accumulation of hydrophobic residues (Phe88, Ile90, Phe141, Ile142, Val158, Phe165, and Phe167) near the top, there is no clear preference for hydrophobic residues on the inside and for hydrophobic residues on the outside (see Figure 1B).

Interactions between the Proregion and the Mature Form. The proregion and the mature part of prostaphopain B are covalently linked, and they form extensive noncovalent contacts that bury a total surface area of 3600 Å^2 (see Figure 2A). Most well-ordered contacts are distant from the active site, and involve the insertion of a staphopain specific loop from Leu375 to Asn385 in the mature form (alignment with other papain-type peptidases not shown) into the interior of the half-barrel formed by the proregion (extra thick lines in Figure 2A). The staphopain specific loop appears to adapt to the presence of the proregion, because it is present in a

[2] The DALI score is a measure of structural similarity between two proteins in standard deviation above the statistically expected similarity.

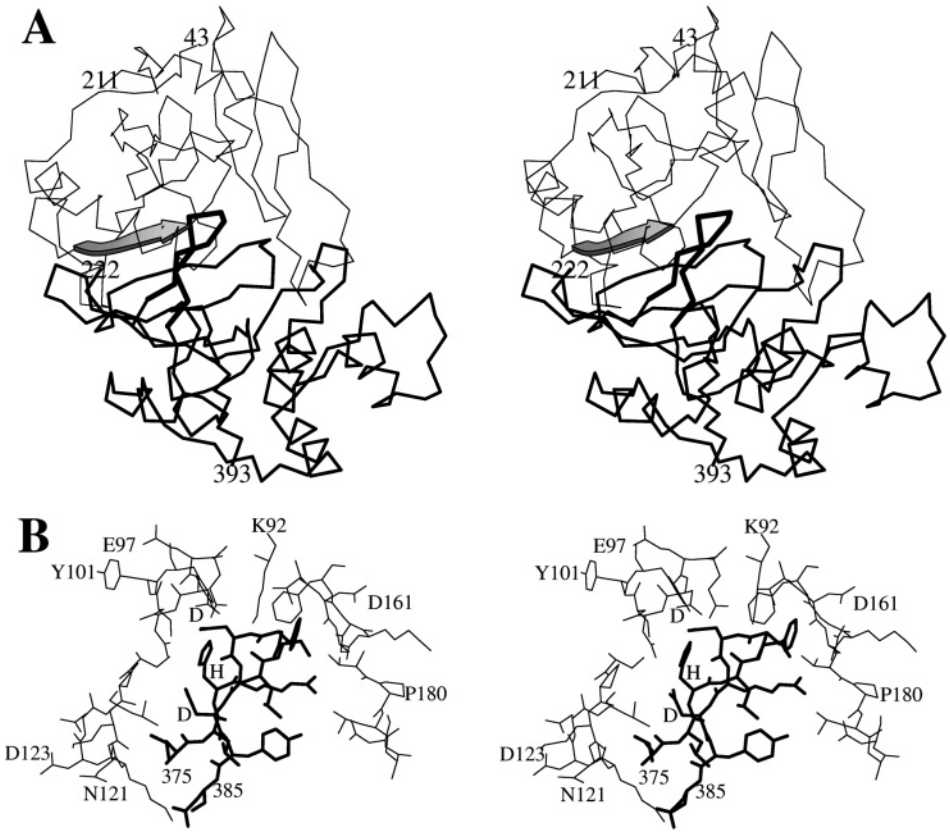

FIGURE 2: Stereodiagrams of the interactions between the proregion of prostaphopain B (thin lines) and the mature form (thick lines). (A) C^{α} trace of prostaphopain B. The edge strand of the proregion that interacts with an edge strand of the mature form is shown in ribbon representation. The staphopain specific loop that inserts into the half-barrel of the proregion is drawn with extra thick lines. (B) The same loop is shown in the identical orientation in an all-atom representation together with residues of the proregion that are <4 Å from it (and with some bridging residues of the proregion that have been included to reduce the number of polypeptide chain fragments in the drawing). Asp98 of the proregion and His377 and Asp383 of the mature form that form two salt bridges have been labeled in the one-letter convention.

different conformation in the staphopain B−staphostatin B complex (superposition not shown). In the prostaphopain structure, it is involved in a number of specific interactions, in particular, the buried salt bridge between Asp98 of the proregion (labeled "D" and drawn as thin lines in Figure 2B) and His377 of the mature form (labeled "H" and drawn as thick lines in Figure 2B). We assume that His377 is protonated so that it can form another salt bridge with Asp383 of the mature form, an interaction that would preorient the imidazole ring for salt bridge formation with the aspartate of the proregion.

The interaction between the proregion and the mature form effectively joins the half-barrel of the proregion and the pseudobarrel of the mature form into one continuous β-sheet, saturating main chain hydrogen bond donors and acceptors in the "edge" (*23*) strand "4" of the proregion (drawn in a ribbon representation in Figure 2A) and in an edge (*23*) strand of the pseudobarrel of the mature protease that would be exposed to solvent in the isolated components.

Occlusion of Primed Substrate Binding Subsites. The proregion blocks the active site cleft only on one side of the nucleophilic cysteine. A comparison of the active site-filling residues of the proregion (see Figure 3A) with the active site-spanning residues of the binding loop of staphostatin B (see Figure 3B) (*13*) shows that the two polypeptide chains run in opposite directions. As the staphostatin B binding loop is known to mimic a substrate (*13*), we conclude that the active site-occluding residues of the proregion bind in the opposite orientation to substrates. A detailed comparison of panels A and B of Figure 3 shows that the side chains of Leu181, Pro180, Thr179, and Ala178 of the proregion are in positions spatially similar to those of the side chains of Thr99, Ser100, Pro102, and Ile103 of the staphostatin B binding loop. As Thr99 and Ser100 in staphostatin B are equivalent to the P1′ and P2′ residues in a substrate, we conclude in Berger's and Schechter's nomenclature (*24*)[3] Leu181 and Pro180 fill the S1′ and S2′ subsites of the protease, respectively. Assignment of further primed subsites is difficult, because Arg101 in staphostatin B has no spatial equivalent in the prostaphopain B structure.

Nonprimed Substrate-Binding Subsites. The prostaphopain B proregion kinks sharply near the active site cysteine to leave all nonprimed substrate binding subsites unoccluded. In prostaphopain B from *S. aureus* strain V8, which was used for this study, the residue at the kink is an alanine. The equivalent residue in prostaphopain B from strain SP6391, which was used in the study by Massimi and colleagues, is a proline (*10*). Although proregions from different strains are more than 96% identical in amino acid sequence, further strain differences occur in the region downstream of the kink that is poorly ordered in all four copies of prostaphopain B in our crystals.

[3] The Schechter and Berger nomenclature refers to substrates as $^{+}H_3N$-...-P2-P1↓P1′-P2′-...-COO^{-} and to the corresponding subsites of the enzyme as S2, S1, S1′, and S2′.

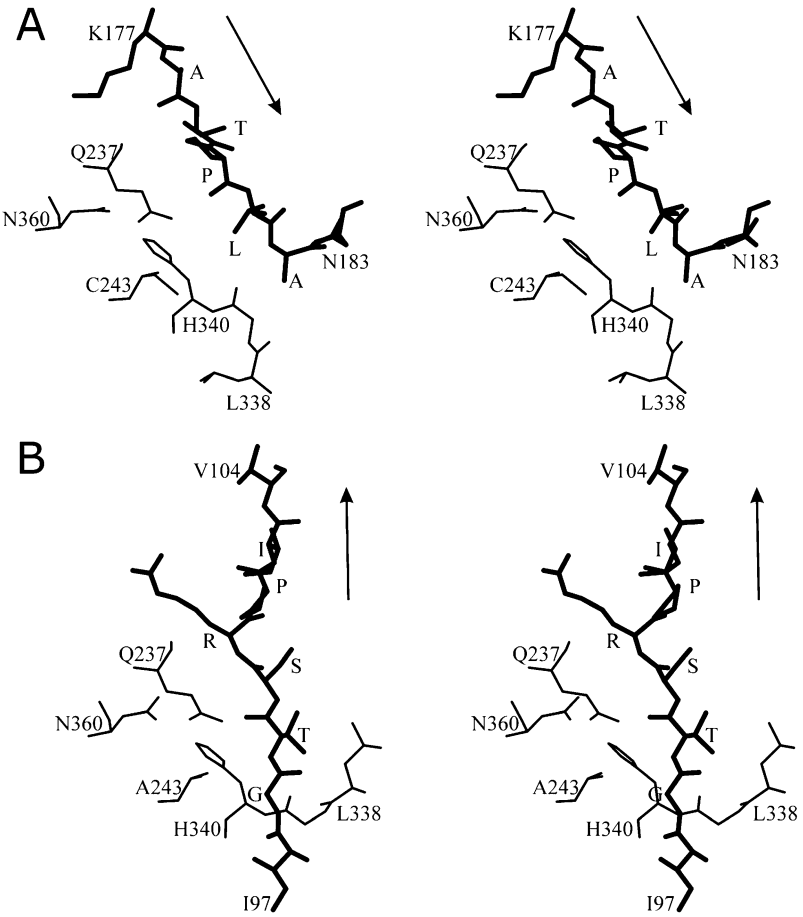

FIGURE 3: Stereodiagram of (A) prostaphopain B proregion residues and (B) staphostatin B residues that insert into the active site cleft of the protease. Only residues of the proregion and of the inhibitor that fill the active site clefts are shown (thick lines), with arrows indicating the directionality of the polypeptide chains. The mature parts of the protease are in the identical orientation, and only selected residues are presented (thin lines). Note that in panel B residue 243 is alanine, because this crystal contained the inactive Cys243Ala mutant of the protease.

Although the proregion does not block nonprimed substrate binding subsites, these sites are not free in our crystals. As the comparison of panels A and B of Figure 3 shows, Leu338 of the mature form of the protease fills the position that P2 residue Ile97 of staphostatin B occupies in the staphopain B−staphostatin B complex. The loss of the previous S2 subsite of the protease results from a major rearrangement of the loop upstream of the catalytic His340. Leu338 is well-defined in one molecule (subunit D in PDB entry 1X9Y), moderately well defined in a second molecule (subunit B in PDB entry 1X9Y), and poorly defined in the other two molecules in the asymmetric unit of the prostaphopain B crystals. Electron density is poor or missing for most residues of the loop upstream of Leu338, raising doubts about the importance of the loss of the S2 subsite of the protease that is observed in the crystals.

Experimentally, soaking prostaphopain B crystals with E-64, an epoxide-based inhibitor of papain-type peptidases, did not result in any defined electron density for the inhibitor, even though the inhibitor would be expected to bind to only nonprimed substrate binding subsites based on its crystallographically characterized mode of binding to mature staphopain A (*25*), probably because it failed to displace Leu338 in the crystal. On the other hand, we had previously observed (J. Potempa, unpublished observation) that binding of a biotin-labeled variant of E-64 to prostaphopain B could be detected in Western blots that, unlike crystallographic soaking experiments, can detect a minority fraction of the proenzyme−inhibitor complex.

The Catalytic Machinery Is Not Significantly Distorted. A distortion of the catalytic machinery in the active site has been suggested as the mechanism for maintaining proenzyme latency in prostreptopain, the inactive precursor of another papain-type peptidase (*9*). Unfortunately, no structure of any uninhibited staphopain molecule is available, but structures of complexes of staphopain A with the epoxide inhibitor E-64 (*25*) and of an inactive Cys243Ala mutant with staphostatin B (*13*) have been determined at high resolution. A superposition of the present proenzyme structure with the protease molecules in these two structures reveals no significant differences in the arrangement of catalytic residues (Cys243, His340, Asn360, and Gln237), at least at the level of accuracy of the 2.5 Å prostaphopain B structure, suggesting that active site distortion is unlikely to play a significant role in maintaining prostaphopain B latency. However, we note that there are significant differences in the loop just upstream of the catalytic histidine. This loop appears to be flexible and is different in all three structures, and differs even between protease molecules in the asymmetric unit of the same crystal (not shown).

The Proregion Has Affinity for the Mature Protease. The large interaction area between the proregion and the mature part of prostaphopain B suggested that there should be substantial affinity between the two parts in the absence of

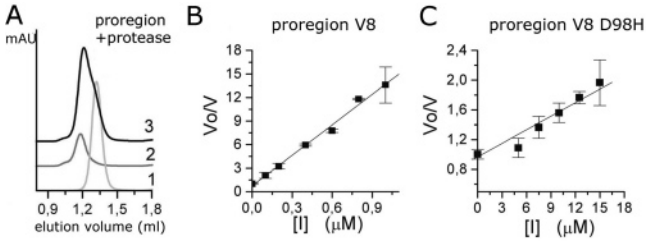

FIGURE 4: Interaction of the proregion and mature form. (A) Gel filtration profiles for staphopain B C243A (trace 1), the proregion (trace 2) and their mixture (trace 3). (B) Determination of the dissociation constant for the proregion and the mature part of prostaphopain B from the V8 strain. (C) Determination of the dissociation constant for the D98H point mutant of the proregion and of the mature part of prostaphopain B from the V8 strain. In panels B and C, 50 nM staphopain B and 1 μM substrate were taken for the assays.

a covalent link. As shown in Figure 4A, a complex can indeed be detected by size exclusion chromatography. If injected alone, mature staphopain B migrates as a monomer (see trace 1). Although it is similar in molecular mass, the proregion runs substantially faster (see trace 2; note that the proregion has a much lower absorption coefficient than mature enzyme). If the two components are co-injected, the peak for mature protease is shifted to a higher molecular mass (see trace 3), suggesting the formation of a complex.

The Proregion Is Inhibitory in Trans. The affinity of the proregion for mature protease and the lack of activity of prostaphopain B suggested that the proregion could act as an inhibitor if supplied in trans, although it was not clear from the crystal structure whether full or partial inhibition should be expected. With the fluorescence-quenched peptide Abz-Gln-Gly-Ile-Gly-Thr-Ser-Arg-Pro-Lys(Dnp)-Asp-OH as the substrate, we find that a large excess of the proregion quenches the proteolytic activity of mature protease entirely (data not shown). From the dependence of the initial velocity of the hydrolysis reaction on the inhibitor concentration, a binding constant of 0.075 $\pm$ 0.002 μM for the affinity between the proregion from strain V8 and the mature protease can be deduced (see Figure 4B). If the experiment is repeated with the proregion from strain NCTC 8325-4 that is identical in sequence to the proregion in the study of Massimi *et al.* (*10*), a binding constant of 0.16 $\pm$ 0.02 μM, or a 2-fold weaker complex, is found.

A Mutation in the Proregion Supports the Crystallographic Binding Mode. The inhibitory properties of the proregion supplied in trans provided an opportunity to test the relevance of the crystallographic binding mode in solution. The buried salt bridge between Asp98 of the proregion and His377 of the mature form (see Figure 2B) is strategically placed at the interface between the proregion and the mature part of prostaphopain B. Mutation of the Asp98 to histidine reduced the affinity of the proregion for the mature part 200-fold to a dissociation constant of 16 $\pm$ 2 μM (see Figure 4C).

A Prostaphopain B−Staphostatin B Complex? There are contradictory reports in the literature about a possible prostaphopain B−staphostatin B complex (*10*, *11*). To test whether formation of such a complex would be compatible with the structural data, we compared the binding modes of the proregion and of staphostatin B to those of mature staphopain B in more detail. As shown in Figure 5, the globular parts of the proregion (see Figure 5A) and of staphostatin B (see Figure 5B) (*13*) bind to mostly nonoverlapping surfaces of the protease. However, modeling of a possible prostaphopain B−staphostatin B complex shows that clashes occur both inside and outside the active site cleft. Clashes within the active site involve residues previously described as equivalent in prostaphopain B and the staphopain B−staphostatin B complex. Clashes outside the active site occur for proregion residues Lys92−Asn94, Asp161−Gly164, and Asn183−Ser195. Remarkably, the clashing parts of the proregion outside the active site are either loop residues or residues that were built into poor electron density and are likely to be mobile in the prostaphopain B structure.

As we could not exclude from the structure the possibility that the clashes in a hypothetical prostaphopain B−staphostatin B complex could be relieved by adaptive fit, we next looked for a possible prostaphopain B−staphostatin B interaction by size exclusion chromatography. As shown in Figure 6A, we could not detect any complex between prostaphopain B and staphostatin B. Although the proregion and staphostatin B would be juxtaposed in a hypothetical complex, we also could not find any indication of the formation of a complex between these two components either (see Figure 6B). However, if the proregion, the inhibitor, and the protease are injected together (see lane 3 of Figure 6C), at least part of the protein migrates faster than either the staphopain B−staphostatin B complex (see lane 1 of Figure 6C) or the staphopain B−proregion complex (see lane 2 of Figure 6C).

DISCUSSION

Proregion Fold. The fold of the proregion is distantly related to a β-barrel. β-Sheet architecture dictates that inward- and outward-pointing residues alternate within each β-stand and occur in register between β-strands, resulting in a characteristic pattern of polar and nonpolar residues in an ideal β-barrel with a hydrophobic core and solvent-exposed exterior (*26*, *27*). The proregion of prostaphopain B corresponds poorly to these expectations for an ideal barrel. The structure is best described as a half-barrel or barrel-sandwich hybrid, because strands 4 and 7 are not connected through main chain hydrogen bonds. This deviation from the ideal barrel architecture leaves the interior far more exposed to solvent, and indeed, many residues that point toward the inside of the barrel (drawn in bold in Figure 1B) are hydrophilic. In contrast to idealized β-barrels, a substantial part of the outer surface of the proregion half-barrel is protected from solvent by additional parts of the structure that are not part of the half-barrel itself. Consequently, a substantial number of residues that point to the outside of the half-barrel (drawn in thin lines in Figure 1B) are hydrophobic.

Proregion−Mature Form Interaction. The 1800 Å^2 interaction area between the proregion and the mature form of prostaphopain B is substantially larger than the 1150 Å^2 interaction area between staphopain B and staphostatin B in the previously described protease−inhibitor complex (*13*). In contrast, the approximately 0.1 μM affinity between the proregion and the mature protease is at least 2 orders of magnitude weaker than the affinity between staphopain B and staphostatin B (*13*) and also relatively low by comparison with the affinities of other proteins that interact through

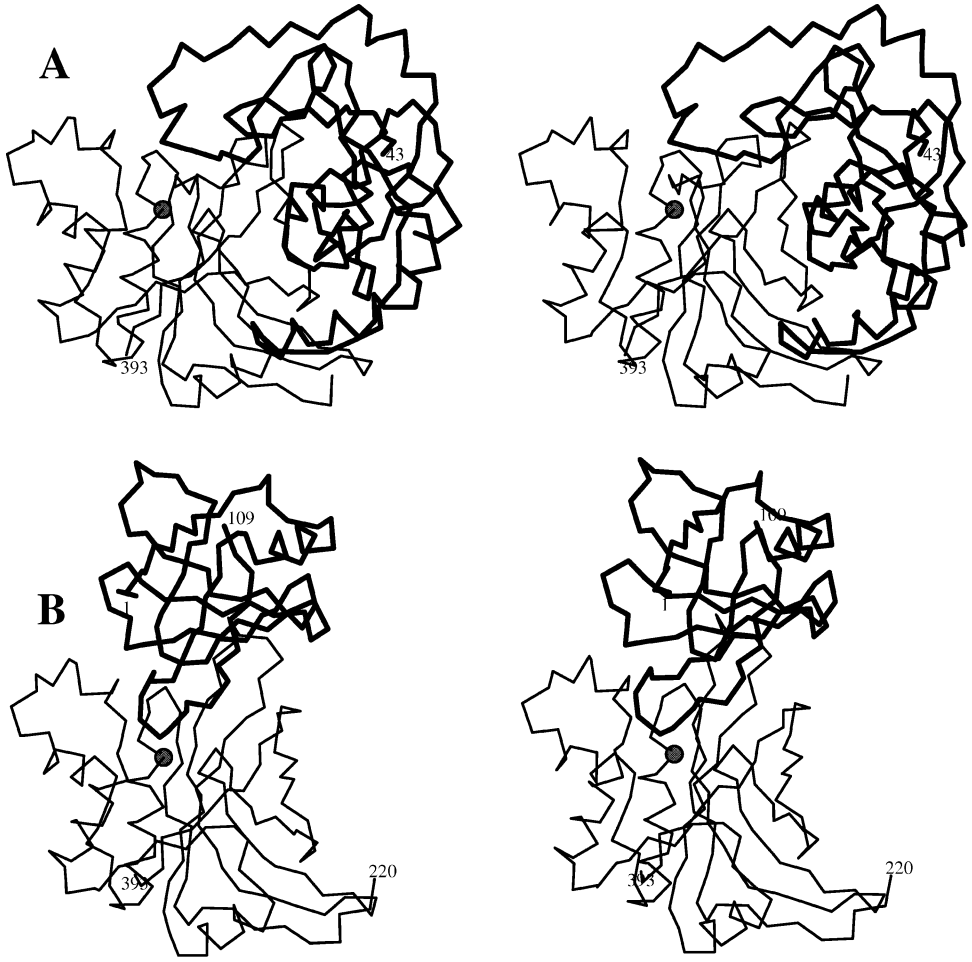

FIGURE 5: Stereo C^{α} trace of (A) prostaphopain B and (B) the staphopain B−staphostatin B complex. The mature forms of the protease are in analogous orientations in both parts of the figure, and are shown as thin lines. The black balls mark the positions of the C^{α} atoms of the active site cysteines. The prostaphopain B proregion in panel A and staphostatin B in panel B are shown with thick lines. Note that in panel B the black balls mark the positions of the C^{α} atoms of alanine, because this crystal contained the inactive Cys243Ala mutant of the protease.

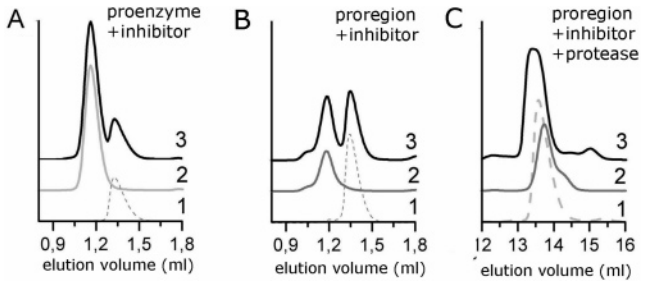

FIGURE 6: Gel filtration profiles for (A) staphostatin B (trace 1), prostaphopain B (trace 2), and their mixture (trace 3), (B) staphostatin B (trace 1), the proregion (trace 2), and their mixture (trace 3), and (C) staphostatin B with staphopain B (trace 1), the proregion with staphopain B (trace 2), and three proteins together (trace 3), all in equimolar amounts. The inactive C243A mutant of the mature protease was used throughout.

interfaces similar in size (*28*). We suspect that the relatively poor affinity is connected with the hydrophilic nature of the contact region. With the exception of a salt bridge at the interface that appears to be very specific and contributes to the affinity (compare panels B and C of Figure 4), most other interactions between the proregion and the mature part could probably be replaced by interactions with solvent, if the components were separated.

Is the Proenzyme Latent? Massimi *et al*. report a 3−4-fold lower specific activity for the proenzyme than for the mature enzyme, but they conclude that the residual activity is significant and, thus, that the proregion does not act as an inhibitor (*10*). In contrast, we find that the proenzyme has at best very residual activity, even after several weeks of storage at 4 °C, and we show quantitatively in this study that a large excess of the proregion can quench the proteolytic activity of the mature form entirely. Originally, we reasoned that this difference may result from the use of different substrates. Massimi *et al*. used Bz-Pro-Phe-Arg-pNA, a substrate that binds predominantly to nonprimed substrate-binding subsites (*10*). In contrast, most experiments for this study were carried out with the fluorescence-quenched substrate Abz-Gln-Gly-Ile-Gly-Thr-Ser-Arg-Pro-Lys(Dnp)-Asp-OH that fills both nonprimed and primed substrate-binding subsites. In light of the crystal structure, it would make sense that proenzyme activity could be detected with the former but not with the latter substrate. In contrast to this expectation, we failed to detect significant proenzyme activity with the proenzyme from strain V8 even with Bz-Pro-Phe-Arg-pNA, suggesting that differences in the purification protocol, differences between native and recombinant enzymes, or differences between the proenzymes from different strains may play a role. We note that a direct

comparison in this study shows that the proregion that was used by Massimi and colleagues has a 2-fold lower affinity for mature protease than the proregion from the V8 strain that was used for the rest of this study, suggesting that the displacement of the S1′ occluding Leu181 to make space for the *p*-nitroanilide may occur more easily in the proenzyme from their strain.

Massimi *et al*. report that prostaphopain B does not mature autocatalytically, even though they can detect activity of the proform with their substrate (*10*). In our hands, with Abz-Gln-Gly-Ile-Gly-Thr-Ser-Arg-Pro-Lys(Dnp)-Asp-OH as the substrate, the specific activity of the proenzyme is low compared to the activity of the mature enzyme even after weeks of storage at 4 °C, strongly supporting the conclusion by Massimi *et al*. that the proenzyme does not autoactivate. In structural terms, at least two features prevent cleavage of the peptide in the active site cleft. First, the polypeptide chain runs in the opposite direction as for substrates, and second, it kinks near the active site cysteine so that no amide bond is in the proper position for productive nucleophilic attack.

Prostaphopain B is efficiently activated by V8 protease *in vitro* and *in vivo* (*10*). The presumed processing sites, several glutamyl−peptidyl amide bonds, are all located in a linker segment that connects the proregion and the mature part of the protease and is disordered in the crystal structure. Lack of order in this region makes biological sense, because it makes the scissile peptide bonds optimally available for V8 processing.

A Complex of Prostaphopain B with Staphostatin B? Massimi *et al*. report that the addition of staphostatin B quenches the activity of prostaphopain B that they can detect with their substrate (*10*). In agreement with Rzychon *et al*. (*11*), we could not detect a prostaphopain B−staphostatin B complex via size exclusion chromatography. However, we observed tentative evidence for complex formation when we injected mature staphostatin B, the proregion of prostaphopain B and staphostatin B together. In this gel filtration run, a fast-migrating species was observed that runs faster than either prostaphopain B or the staphopain B−staphostatin B complex. On the basis of our data, a prostaphopain B−staphostatin B complex is possible, but either it would have to be a weak complex or it would have to depend on special conditions. We also cannot exclude the possibility that a stronger complex would be formed with the proenzyme from the strain that was used in the study by Massimi *et al*., or that it would require the use of native rather than recombinant protein components.

Prostaphopain B versus Proforms of Other Papain-Type Peptidases. The similarity between mature staphopain B and other papain-type peptidases is readily apparent. In contrast, there is no structural similarity between the proregions of prostaphopain B and procathepsin L (*3*), procathepsin B (*2*, *5*), procaricain (*4*), procathepsin K (*6*, *7*), or prostreptopain (*9*). Despite these differences, all proregions keep the mature form in a latent state, and they act as inhibitors if supplied in trans.

The interaction between the proregion and the mature form of prostaphopain B is unusual in at least three ways. First, the interaction surface extends over 1800 Å^2, a value larger than that for any procathepsin, and most of this surface is located far from the active site. Second, and despite the large interaction area, the affinity between the proregion and the mature form of prostaphopain B is lower than between the corresponding components of procathepsins (*29*−*31*). Third, none of the active site cleft-occluding residues of prostaphopain B is part of a helix, as would be typical for at least some of the active site cleft-occluding residues in the proforms of other papain-type peptidases (*3*, *5*, *6*).

The binding of the proregion to the active site cleft in the opposite orientation as substrates is not unusual for the proforms of papain-type peptidases, and has previously been observed in the crystal structures of procathepsin B (*2*, *5*), procathepsin L (*3*), and procaricain (*4*) or procathepsin K (*6*, *7*). In these structures, "backward" binding explains the resistance of the active site-spanning residues of the proregion to proteolytic cleavage. In prostaphopain B, this feature is combined with the kink in the proregion that prevents the exposure of any scissile peptide bond to the cysteine nucleophile in the active site. To the best of our knowledge, a similarly sharp bend in the active site-directed part of the proregion has so far only been observed in the procathepsin X crystal structure (*8*). Despite this similarity, the prostaphopain B and procathepsin X latency mechanisms are very different. In procathepsin X, the proregion occludes the nonprimed substrate binding subsites of the protease but does not interact with the primed sites. In contrast, only primed substrate binding subsites are directly occluded by the proregion in the prostaphopain B model. Moreover, there is a unique disulfide bond between a cysteine residue of the proregion and the active site cysteine of the mature enzyme in procathepsin X that has no counterpart in other proenzymes of papain-like peptidases, including prostaphopain B.

A Prostaphopain B−Staphostatin B Complex Would Be Unusual, but Not without Precedent. Very recent biochemical work has shown that procathepsin L can bind to its endogenous protein inhibitors, the cystatins, without prior proteolytic removal of the propeptide. This occurs only when the propeptide is displaced from the active site by denaturation at low pH or in the presence of molecules that preferentially bind to the unfolded proregion. It has been suggested that in this case binding of the inhibitor to the proenzyme increases the susceptibility of the proregion to cleavage (*32*). For the prostaphopain B−staphostatin B system, our data demonstrate that proenzyme cleavage enhances the affinity for staphostatin B, but clearly, more work is required to elucidate the interplay of prostaphopain B, staphopain B, and staphostatin B *in vitro* and *in vivo.*

ACKNOWLEDGMENT

We thank Hans Bartunik for generous allocation of beamtime on BW6/DESY and G. Bourenkov and G. Kachalova for assistance during data collection. We are grateful for access to the protein crystallography beamlines in EMBL Hamburg, and especially to Paul Tucker, Hendrik Zwart, and Elzbieta Nowak for help during data collection on the EMBL beamlines. We are grateful to David Drechsel and Tim Noetzel for access to and help with an Ettan chromatography system and to the members of the Warsaw Structural Biology group for a critical reading of the manuscript. We thank Aneta Oleksy from the Department of Microbiology, Faculty of Biotechnology, Jagiellonian University, for purifying staphylococcal proteinases.

REFERENCES

1. Groves, M. R., Coulombe, R., Jenkins, J., and Cygler, M. (1998) Structural basis for specificity of papain-like cysteine protease proregions toward their cognate enzymes, *Proteins 32*, 504−514.
2. Cygler, M., Sivaraman, J., Grochulski, P., Coulombe, R., Storer, A. C., and Mort, J. S. (1996) Structure of rat procathepsin B: model for inhibition of cysteine protease activity by the proregion, *Structure 4*, 405−416.
3. Coulombe, R., Grochulski, P., Sivaraman, J., Menard, R., Mort, J. S., and Cygler, M. (1996) Structure of human procathepsin L reveals the molecular basis of inhibition by the prosegment, *EMBO J. 15*, 5492−5503.
4. Groves, M. R., Taylor, M. A., Scott, M., Cummings, N. J., Pickersgill, R. W., and Jenkins, J. A. (1996) The prosequence of procaricain forms an α-helical domain that prevents access to the substrate-binding cleft, *Structure 4*, 1193−1203.
5. Podobnik, M., Kuhelj, R., Turk, V., and Turk, D. (1997) Crystal structure of the wild-type human procathepsin B at 2.5 Å resolution reveals the native active site of a papain-like cysteine protease zymogen, *J. Mol. Biol. 271*, 774−788.
6. LaLonde, J. M., Zhao, B., Janson, C. A., D'Alessio, K. J., McQueney, M. S., Orsini, M. J., Debouck, C. M., and Smith, W. W. (1999) The crystal structure of human procathepsin K, *Biochemistry 38*, 862−869.
7. Sivaraman, J., Lalumiere, M., Menard, R., and Cygler, M. (1999) Crystal structure of wild-type human procathepsin K, *Protein Sci. 8*, 283−290.
8. Sivaraman, J., Nagler, D. K., Zhang, R., Menard, R., and Cygler, M. (2000) Crystal structure of human procathepsin X: a cysteine protease with the proregion covalently linked to the active site cysteine, *J. Mol. Biol. 295*, 939−951.
9. Kagawa, T. F., Cooney, J. C., Baker, H. M., McSweeney, S., Liu, M., Gubba, S., Musser, J. M., and Baker, E. N. (2000) Crystal structure of the zymogen form of the group A *Streptococcus* virulence factor SpeB: an integrin-binding cysteine protease, *Proc. Natl. Acad. Sci. U.S.A. 97*, 2235−2240.
10. Massimi, I., Park, E., Rice, K., Muller-Esterl, W., Sauder, D., and McGavin, M. J. (2002) Identification of a novel maturation mechanism and restricted substrate specificity for the SspB cysteine protease of *Staphylococcus aureus*, *J. Biol. Chem. 277*, 41770−41777.
11. Rzychon, M., Sabat, A., Kosowska, K., Potempa, J., and Dubin, A. (2003) Staphostatins: an expanding new group of proteinase inhibitors with a unique specificity for the regulation of staphopains, *Staphylococcus* spp. cysteine proteinases, *Mol. Microbiol. 49*, 1051−1066.
12. Rzychon, M., Filipek, R., Sabat, A., Kosowska, K., Dubin, A., Potempa, J., and Bochtler, M. (2003) Staphostatins resemble lipocalins, not cystatins in fold, *Protein Sci. 12*, 2252−2256.
13. Filipek, R., Rzychon, M., Oleksy, A., Gruca, M., Dubin, A., Potempa, J., and Bochtler, M. (2003) The staphostatin−staphopain complex: a forward binding inhibitor in complex with its target cysteine protease, *J. Biol. Chem. 278*, 40959−40966.
14. Vagin, A., and Teplyakov, A. (2000) An approach to multi-copy search in molecular replacement, *Acta Crystallogr. D56* (Part 12), 1622−1624.
15. Levitt, D. G. (2001) A new software routine that automates the fitting of protein X-ray crystallographic electron-density maps, *Acta Crystallogr. D57*, 1013−1019.
16. Potterton, E., Briggs, P., Turkenburg, M., and Dodson, E. (2003) A graphical user interface to the CCP4 program suite, *Acta Crystallogr. D59*, 1131−1137.
17. Jones, T. A., Zou, J. Y., Cowan, S. W., and Kjeldgaard, M. (1991) Improved methods for building protein models in electron density maps and the location of errors in these models, *Acta Crystallogr. A47* (Part 2), 110−119.
18. Perrakis, A., Morris, R., and Lamzin, V. S. (1999) Automated protein model building combined with iterative structure refinement, *Nat. Struct. Biol. 6*, 458−463.
19. Brunger, A. T., Adams, P. D., Clore, G. M., DeLano, W. L., Gros, P., Grosse-Kunstleve, R. W., Jiang, J. S., Kuszewski, J., Nilges, M., Pannu, N. S., Read, R. J., Rice, L. M., Simonson, T., and Warren, G. L. (1998) Crystallography & NMR system: A new software suite for macromolecular structure determination, *Acta Crystallogr. D54* (Part 5), 905−921.
20. Lee, B., and Richards, F. M. (1971) The interpretation of protein structures: estimation of static accessibility, *J. Mol. Biol. 55*, 379−400.
21. Holm, L., and Sander, C. (1995) Dali: a network tool for protein structure comparison, *Trends Biochem. Sci. 20*, 478−480.
22. Murzin, A. G., Brenner, S. E., Hubbard, T., and Chothia, C. (1995) SCOP: a structural classification of proteins database for the investigation of sequences and structures, *J. Mol. Biol. 247*, 536−540.
23. Richardson, J. S., and Richardson, D. C. (2002) Natural β-sheet proteins use negative design to avoid edge-to-edge aggregation, *Proc. Natl. Acad. Sci. U.S.A. 99*, 2754−2749.
24. Schechter, I., and Berger, A. (1967) On the size of the active site in proteases. I. Papain, *Biochem. Biophys. Res. Commun. 27*, 157−162.
25. Hofmann, B., Schomburg, D., and Hecht, H. J. (1993) Crystal Structure of a Thiol Proteinase from *Staphylococcus aureus* V-8 in the E-64 Inhibitor Complex, *Acta Crystallogr. 49* (Suppl.), 102.
26. Murzin, A. G., Lesk, A. M., and Chothia, C. (1994) Principles determining the structure of β-sheet barrels in proteins. I. A theoretical analysis, *J. Mol. Biol. 236*, 1369−1381.
27. Murzin, A. G., Lesk, A. M., and Chothia, C. (1994) Principles determining the structure of β-sheet barrels in proteins. II. The observed structures, *J. Mol. Biol. 236*, 1382−1400.
28. Tsai, C. J., Lin, S. L., Wolfson, H. J., and Nussinov, R. (1997) Studies of protein−protein interfaces: a statistical analysis of the hydrophobic effect, *Protein Sci. 6*, 53−64.
29. Guay, J., Falgueyret, J. P., Ducret, A., Percival, M. D., and Mancini, J. A. (2000) Potency and selectivity of inhibition of cathepsin K, L and S by their respective propeptides, *Eur. J. Biochem. 267*, 6311−6318.
30. Fox, T., de Miguel, E., Mort, J. S., and Storer, A. C. (1992) Potent slow-binding inhibition of cathepsin B by its propeptide, *Biochemistry 31*, 12571−12576.
31. Carmona, E., Dufour, E., Plouffe, C., Takebe, S., Mason, P., Mort, J. S., and Menard, R. (1996) Potency and selectivity of the cathepsin L propeptide as an inhibitor of cysteine proteases, *Biochemistry 35*, 8149−8157.
32. Majerle, A., and Jerala, R. (2003) Protein inhibitors form complexes with procathepsin L and augment cleavage of the propeptide, *Arch. Biochem. Biophys. 417*, 53−58.

BI048661M